

Magnetic cycles of the planet-hosting star τ Bootis *

J.-F. Donati¹†, C. Moutou², R. Farès¹, D. Bohlender³, C. Catala⁴, M. Deleuil²,
E. Shkolnik⁵, A.C. Cameron⁶, M.M. Jardine⁶, G.A.H. Walker⁷

¹ *LATT-UMR 5572, CNRS & Univ. P. Sabatier, 14 Av. E. Belin, F-31400 Toulouse, France*

² *LAM-UMR 6110, CNRS & Univ. de Provence, Traverse du Siphon, F-13376 Marseille, France*

³ *HIA/NRC, 5071 West Saanich Road, Victoria, BC V9E 2E7, Canada*

⁴ *LESIA-UMR 8109, CNRS & Univ. Paris VII, 5 Place Janssen, F-92195 Meudon Cedex, France*

⁵ *NASA Astrobiology Institute, Univ. of Hawaii at Manoa, 2680 Woodlawn Drive, Honolulu, HI 96822, USA*

⁶ *School of Physics and Astronomy, Univ. of St Andrews, St Andrews, Scotland KY16 9SS, UK*

⁷ *1234 Hewlett Place, Victoria, BC V8S 497, Canada*

2007, MNRAS, submitted

ABSTRACT

We have obtained new spectropolarimetric observations of the planet-hosting star τ Bootis, using the ESPaDOnS and NARVAL spectropolarimeters at the Canada-France-Hawaii Telescope (CFHT) and Telescope Bernard-Lyot (TBL).

With this data set, we are able to confirm the presence of a magnetic field at the surface of τ Boo and map its large-scale structure over the whole star. The large-scale magnetic field is found to be fairly complex, with a strength of up to 10 G; it features a dominant poloidal field and a small toroidal component, the poloidal component being significantly more complex than a dipole. The overall polarity of the magnetic field has reversed with respect to our previous observation (obtained a year before), strongly suggesting that τ Boo is undergoing magnetic cycles similar to those of the Sun. This is the first time that a global magnetic polarity switch is observed in a star other than the Sun; given the unfrequent occurrence of such events in the Sun, we speculate that the magnetic cycle period of τ Boo is much shorter than that of the Sun.

Our new data also allow us to confirm the presence of differential rotation, both from the shape of the line profiles and from the latitudinal shearing that the magnetic structure is undergoing. The differential rotation surface shear that τ Boo experiences is found to be 6 to 10 times larger than that of the Sun, in good agreement with recent claims that differential rotation is strongest in stars with shallow convective zones. We propose that the short magnetic cycle period is due to the strong level of differential rotation.

With a rotation period of 3.0 and 3.9 d at the equator and pole respectively, τ Boo appears as the first planet-hosting star whose rotation (at intermediate latitudes) is synchronised with the orbital motion of its giant planet (period 3.3 d). Assuming that this synchronisation is not coincidental, it suggests that the tidal effects induced by the giant planet can be strong enough to force the thin convective envelope (though not the whole star) into corotation.

We also detect time dependent activity fluctuations on τ Boo, but cannot unambiguously determine whether they are intrinsic to the star or induced by the planet; more observations of similar type are needed to determine the role of the close-in giant planet orbiting τ Boo on both the activity enhancements and the magnetic cycle of the host star.

Key words: stars: magnetic fields – stars: planetary systems – stars: activity – stars: individual: τ Boo – techniques: spectropolarimetry

† Based on observations obtained with ESPaDOnS at the Canada-France-Hawaii Telescope (CFHT) and with NARVAL at

1 INTRODUCTION

Magnetic fields of stars hosting close-in giant planets have recently started to trigger a lot of interest from the astrophysical community. Magnetic fields on the host star are indeed likely to play a direct role in the survival of close-in giant planets. By evacuating the central regions of their protoplanetary discs (within 0.1 AU from the star typically, Romanova & Lovelace e.g., 2006), magnetic fields of young protostars are generating ideal conditions for giant planets to stop their inward migration whenever they enter the central gap of the disc, leaving them at a location where many close-in giant planets (making up 20% of all known exoplanets to date) are actually observed.

Magnetic fields of stars hosting close-in giant planets are also expected to be a key point in the way such planets interact with their host stars, and numerous studies have been carried out recently to study the details of this interaction. Observations suggest that stars hosting close-in giant planets exhibit enhanced activity correlating with the orbital phase of the planet rather than with the rotation phase of the star, arguing that this increased activity is induced by the presence of the planet (e.g., Shkolnik et al. 2003, 2005); recent observations even suggest that these star-planet interactions could be cyclic in nature and oscillate between ‘on’ and ‘off’ states (Shkolnik et al. 2008). Theoretical studies (e.g., Cuntz et al. 2000; McIvor et al. 2006) propose that this interaction could either result from tidal effects (e.g., enhancing turbulence and hence local dynamo action and activity within the planet-induced tidal bulge) or from magnetospheric interaction (e.g., inducing reconnection events as the planet travels through the large magnetospheric loops of the host star).

For such studies, τ Boo (HR 5185, HD 120136, F7V) is an interesting candidate. Its massive planet is orbiting at 0.049 AU in 3.31 d (e.g., Leigh et al. 2003). Clear Zeeman signatures have recently been detected on τ Boo with the ESPaDOnS spectropolarimeter on the 3.6m Canada-France-Hawaii Telescope (CFHT), demonstrating that a large-scale field of a few G is present at the surface (Catala et al. 2007). Despite its relatively short rotation period (of order 3 d, Henry et al. 2000; Catala et al. 2007), the activity of τ Boo is only moderate (as usual for mid F stars) and shows no strong modulation with either orbital or rotation phase (Shkolnik et al. 2005, 2008); the near synchronisation between the star’s rotation and the planet orbit may explain this lack of planet-induced activity. τ Boo nonetheless appears as a good laboratory for studying and modelling the magnetic fields of stars with close-in giant planets, and in particular those of F stars with shallow convective zones and

the T lescope Bernard Lyot (TBL). CFHT/ESPaDOnS are operated by the National Research Council of Canada, the Institut National des Sciences de l’Univers of the Centre National de la Recherche Scientifique (INSU/CNRS) of France, and the University of Hawaii, while TBL/NARVAL are operated by INSU/CNRS.

† E-mail: donati@ast.obs-mip.fr (J-FD); claire.moutou@oamp.fr (CM); rim.fares@ast.obs-mip.fr (RF); david.bohlender@nrc-cnrc.gc.ca (DB); claude.catala@obspm.fr (CC); magali.deleuil@oamp.fr (MD); shkolnik@ifa.hawaii.edu (ES); acc4@st-andrews.ac.uk (ACC); mmj@st-andrews.ac.uk (MMJ) gordonwa@uvic.ca (GAHW)

low intrinsic activity on which the (presumably very small) planet-induced activity enhancements are easier to detect.

We present in the paper a detailed modelling of the magnetic field and differential rotation at the surface of τ Boo, as a follow-up study from the initial discovery of Catala et al. (2007). Sec. 2 presents the observations, Sec. 3 details the magnetic and differential rotation modelling while Sec. 4 provides a discussion and future prospects about this work.

2 OBSERVATIONS

For these renewed observations, we used again the ESPaDOnS spectropolarimeter (Donati et al., in preparation) on CFHT; we also collected a few additional polarised spectra with NARVAL on the 2m T lescope Bernard Lyot (TBL). Both instruments yield a spectral resolution of about 65,000. Each spectrum consists of a sequence of 4 individual subexposures taken in different configurations of the polarimeter retarders, in order to perform a precise and achromatic circular polarisation analysis and suppress all spurious signatures at first order (Donati et al. 1997, Donati et al., in preparation).

Data were reduced with the dedicated automatic reduction tool Libre-ESpRIT installed at CFHT and TBL (Donati et al. 1997, Donati et al., in preparation), and changed into sets of Stokes I and V spectra. All spectra are automatically corrected from spectral shifts resulting from instrumental effects (eg mechanical flexures, temperature or pressure variations) using telluric lines as a reference. Though not perfect, this procedure allows spectra to be secured with a radial velocity (RV) precision of about 15–20 m s^{-1} (e.g., Catala et al. 2007; Moutou et al. 2007).

A total of 32 spectra were collected in 2007 June and July in variable weather conditions, mostly with ESPaDOnS/CFHT. The complete log is given in Table 1. All data are phased with the same orbital ephemeris as that of Catala et al. (2007):

$$T_0 = \text{HJD } 2,453,450.984 + 3.31245E \quad (1)$$

with phase 0.0 denoting the first conjunction (i.e., with the planet farthest from the observer). Circularly polarised spectra of stars with stable magnetic topologies (e.g., chemically peculiar stars and hotter equivalents, like τ Sco, Donati et al. 2006) were observed during both runs to check that the instrument behaves properly and yields nominal field strengths and polarities.

Least-Squares Deconvolution (LSD, Donati et al. 1997) was applied to all spectra to retrieve average unpolarised and circularly polarised profiles of photospheric spectral lines. The line pattern used for this process is derived from a Kurucz model atmosphere with solar abundances, and effective temperature and logarithmic gravity set to 6250 K and 4.0 respectively; this line pattern includes most moderate to strong lines present in the optical domain (those featuring central depths larger than 40% of the local continuum, before any macroturbulent or rotational broadening, about 4,000 throughout the whole spectral range) but excludes the very strongest, broadest features, such as Balmer lines, whose Zeeman signature is strongly smeared out compared to those of narrow lines. The typical multiplex gain

Table 1. Journal of observations. Columns 1–6 sequentially list the UT date, the instrument used, the heliocentric Julian date and UT time (both at mid-exposure), the complete exposure time and the peak signal to noise ratio (per 2.6 km s^{-1} velocity bin) of each observation. Column 7 lists the rms noise level (relative to the unpolarized continuum level I_c and per 1.8 km s^{-1} velocity bin) in the circular polarization profile produced by Least-Squares Deconvolution (LSD), while column 8 and 9 list the orbital cycle (using the ephemeris given by Eq. 1) and the radial velocity (RV) associated with each exposure.

Date (2007)	Instrument	HJD (2,453,000+)	UT (h:m:s)	t_{exp} (s)	S/N	σ_{LSD} ($10^{-4}I_c$)	Cycle (245+)	v_{rad} (km s^{-1})
Jun 12	NARVAL/TBL	1264.45160	22:46:05	4×600	1,000	0.37	0.5788	-16.506
Jun 19	NARVAL/TBL	1271.42056	22:02:04	4×600	910	0.42	2.6827	-16.708
Jun 26	ESPaDOs/CFHT	1277.74494	05:49:50	4×300	1,550	0.23	4.5920	-16.589
Jun 26	ESPaDOs/CFHT	1277.81018	07:23:47	4×300	1,730	0.18	4.6117	-16.645
Jun 27	ESPaDOs/CFHT	1278.74598	05:51:27	4×200	1,700	0.21	4.8942	-16.644
Jun 27	ESPaDOs/CFHT	1278.75739	06:07:53	4×200	1,670	0.21	4.8976	-16.641
Jun 27	ESPaDOs/CFHT	1278.76861	06:24:02	4×200	1,710	0.21	4.9010	-16.625
Jun 28	ESPaDOs/CFHT	1279.73666	05:38:08	4×200	1,620	0.22	5.1933	-15.927
Jun 28	ESPaDOs/CFHT	1279.74787	05:54:17	4×200	1,660	0.22	5.1966	-15.915
Jun 28	ESPaDOs/CFHT	1279.75913	06:10:30	4×200	1,730	0.21	5.2000	-15.912
Jun 30	ESPaDOs/CFHT	1281.83298	07:57:04	4×200	1,470	0.25	5.8261	-16.746
Jun 30	ESPaDOs/CFHT	1281.84420	08:13:13	4×200	1,290	0.28	5.8295	-16.739
Jul 01	ESPaDOs/CFHT	1282.73612	05:37:41	4×200	1,640	0.21	6.0988	-16.070
Jul 01	ESPaDOs/CFHT	1282.74732	05:53:49	4×200	1,640	0.21	6.1022	-16.062
Jul 01	ESPaDOs/CFHT	1282.75863	06:10:06	4×200	1,720	0.21	6.1056	-16.058
Jul 02	ESPaDOs/CFHT	1283.73836	05:41:01	4×200	740	0.44	6.4013	-16.093
Jul 02	ESPaDOs/CFHT	1283.74973	05:57:24	4×200	580	0.53	6.4048	-16.090
Jul 02	ESPaDOs/CFHT	1283.76769	06:23:16	4×200	1,240	0.31	6.4102	-16.103
Jul 02	ESPaDOs/CFHT	1283.78209	06:43:60	4×200	1,360	0.27	6.4145	-16.110
Jul 02	ESPaDOs/CFHT	1283.91960	10:02:02	4×300	1,370	0.29	6.4561	-16.193
Jul 03	ESPaDOs/CFHT	1284.74158	05:45:46	4×300	1,370	0.24	6.7042	-16.816
Jul 03	ESPaDOs/CFHT	1284.75763	06:08:53	4×300	1,830	0.19	6.7090	-16.818
Jul 03	ESPaDOs/CFHT	1284.77363	06:31:56	4×300	1,750	0.21	6.7139	-16.808
Jul 03	ESPaDOs/CFHT	1284.85319	08:26:30	4×300	1,700	0.23	6.7379	-16.817
Jul 04	ESPaDOs/CFHT	1285.79220	06:58:47	4×300	1,090	0.33	7.0214	-16.275
Jul 04	ESPaDOs/CFHT	1285.80803	07:21:35	4×300	1,470	0.26	7.0262	-16.248
Jul 04	ESPaDOs/CFHT	1285.86573	08:44:40	4×300	1,240	0.32	7.0436	-16.191
Jul 04	ESPaDOs/CFHT	1285.88171	09:07:41	4×300	990	0.41	7.0484	-16.173
Jul 05	ESPaDOs/CFHT	1286.74025	05:44:05	4×200	330	1.18	7.3076	-15.943
Jul 05	ESPaDOs/CFHT	1286.75144	06:00:12	4×200	250	1.57	7.3110	-15.933
Jul 05	ESPaDOs/CFHT	1286.76265	06:16:20	4×200	310	1.28	7.3143	-15.930
Jul 05	ESPaDOs/CFHT	1286.78415	06:47:18	4×600	400	0.98	7.3208	-15.941

in S/N for polarisation profiles is about 25 to 30, implying noise levels in LSD polarisation profiles as low as 20 ppm (i.e., 2×10^{-5} in units of the unpolarised continuum) in good weather conditions. Zeeman signatures, whenever detected, have a typical amplitude of about 100 ppm (see below).

Radial velocities are obtained from Gaussian fits to each LSD unpolarised profile of τ Boo. We find that our measurements are in good agreement with previous measurements (see Fig. 1). Residuals (rms) with respect to the predicted RV curve are equal to 20 m s^{-1} , i.e., similar to the uncertainties of $15\text{--}20 \text{ m s}^{-1}$ reported by Catala et al. (2007) and Moutou et al. (2007). All Stokes I and V profiles used in the following were corrected for the orbital motion, i.e., translated into the velocity rest frame of τ Boo.

As in Catala et al. (2007), we assume that τ Boo rotates about an axis inclined at an angle $i = 40^\circ$ with respect to the line-of-sight. The unpolarised spectral lines are significantly broadened by rotation and suggest that the rotation of the star is more or less synchronised with the planet orbital motion, i.e., corresponds to a rotation rate of 1.9 rad d^{-1} . By averaging all Stokes I LSD profiles into a single mean line and computing its Fourier transform,

one can estimate the amount of differential rotation at the surface of the star (Reiners & Schmitt 2002). This experiment, first carried out by Reiners (2006) and repeated by Catala et al. (2007), demonstrates that τ Boo is indeed differentially rotating, with a relative differential rotation (i.e., an angular rotation shear relative to the mean angular rotation rate) of 18–20% and an angular rotation shear¹ of $0.35 \pm 0.10 \text{ rad d}^{-1}$; the corresponding rotation periods at the equator and the pole are equal to about 3.0 d and 3.7 d respectively, bracketing the planet orbital period of 3.3 d. The Fourier transform of the average LSD Stokes I profile derived from our new data (not shown here) is very similar to that shown in Catala et al. (2007) (their Fig. 1) and confirms their analysis.

¹ The angular rotation shear derived by Reiners (2006), equal to $0.31 \pm 0.13 \text{ rad d}^{-1}$, is actually scaled down by $\sqrt{\sin i}$; using $i = 40^\circ$, it translates into a true angular rotation shear of $0.38 \pm 0.16 \text{ rad d}^{-1}$ in good agreement with our own estimate.

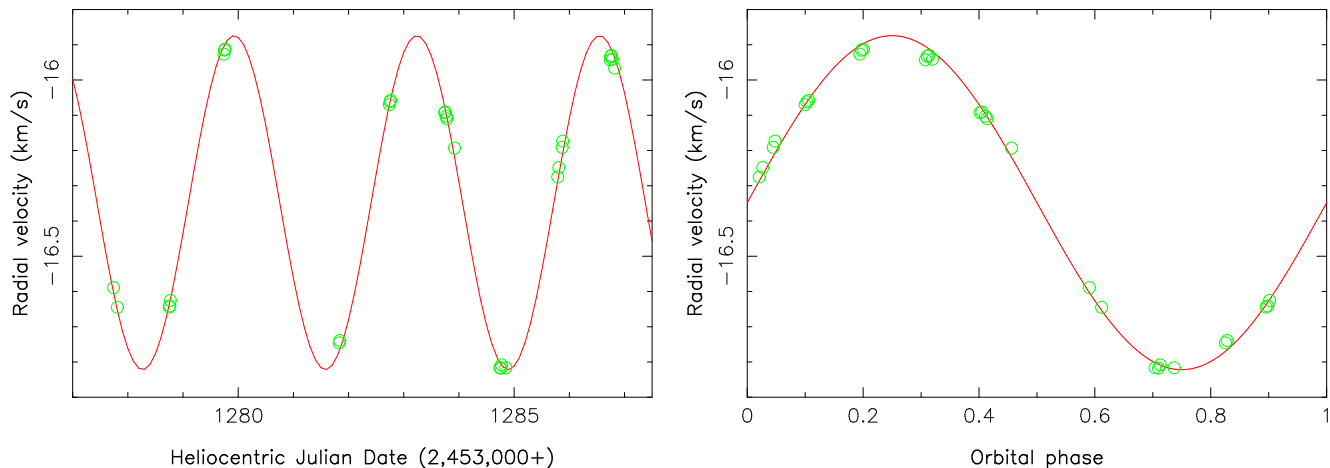


Figure 1. Radial velocities of τ Boo derived from our ESPaDOnS spectra (green circles) as a function of Heliocentric Julian Date (left) and orbital phase (right, using the ephemeris of eq. 1). The radial velocity model plotted here (red full line) corresponds to a circular orbit with an (assumed) velocity semi-amplitude of 467 m s^{-1} (Butler et al. 1997) and a (fitted) systemic velocity of $-16.348 \text{ km s}^{-1}$. Individual error bars on data points ($15\text{--}20 \text{ m s}^{-1}$) are about as large as the symbol size.

3 MAGNETIC MODELLING

3.1 Model description

To model the magnetic topology of τ Boo, we use the new imaging code of Donati et al. (2006) where the field topology is described through spherical-harmonics expansions. We use the principles of maximum entropy image reconstruction to retrieve the simplest magnetic image compatible with the series of rotationally modulated Zeeman signatures. More specifically, the field is divided into its radial-poleoidal, non-radial-poleoidal and toroidal components, each of them described as a spherical-harmonics expansion; given the different rotational modulation of Zeeman signatures that poleoidal and toroidal fields generate, our imaging code appears particularly useful and efficient at producing dynamo-relevant diagnostics about the large-scale magnetic topologies at the surface of late-type stars. One of the latest application of this code can be found in Morin et al. (2007).

The reconstruction process is iterative and proceeds by comparing at each step the synthetic profiles corresponding to the current image with those of the observed data set. To compute the synthetic Zeeman signatures, we divide the surface of the star into small grid cells (typically a few thousands), work out the specific contribution of each grid cell to the Stokes V profiles (given the magnetic field strength and orientation within each grid cell, as well as the cell radial velocity, location and projected area) and finally sum up contributions of all cells. Since the problem is partly ill-posed, we stabilise the inversion process by using an entropy criterion (applied to the spherical harmonics coefficients) aimed at selecting the image with minimum information among all those compatible with the data (Morin et al. 2007).

The model we use to describe the local Stokes I and V profiles is quite simple. While the local unpolarised profile is given by a Gaussian, the local circular polarisation profile is computed assuming the weak field approximation, i.e., that V is proportional to $dI/d\lambda$ and to the local line-of-sight component of the magnetic field (e.g., Donati et al. 1997). Assuming a line-of-sight projected equatorial rotation velocity $v \sin i$ of 15.9 km s^{-1} and a relative differential rotation

of 18%, we obtain synthetic Stokes I profiles whose first 2 zeros in the Fourier transform match those of the observed data; setting the full width at half maximum of the local Stokes I profile to 11 km s^{-1} produces a very good fit to the average Stokes I LSD profiles. This simple line model was used quite extensively and has proved to be efficient at correctly reproducing observed sets of rotationally modulated Zeeman signatures (e.g., Catala et al. 2007; Moutou et al. 2007).

To incorporate differential rotation into the modelling, we proceed as in Donati et al. (2003) and Morin et al. (2007), i.e., by assuming that the rotation rate at the surface of the star is varying with latitude θ as $\Omega_{\text{eq}} - d\Omega \sin^2 \theta$ where Ω_{eq} is the rotation rate at the equator $d\Omega$ the difference in rotation rate between the equator and the pole. When computing the synthetic profiles, we use this law to work out the longitude shift of each cell at each observing epoch with respect to its location at the median observing epoch (at which the field is reconstructed, i.e., orbital cycle $6 + 245 = 251$ in the present case and in the ephemeris of eq. 1 or HJD 2,454,282.41) so that we can correctly evaluate the true spectral contributions of all cells at all epochs.

For each pair of Ω_{eq} and $d\Omega$ values within a range of acceptable values, we then derive, from the complete data set, the corresponding magnetic topology (at a given information content) and the associated reduced chisquare level χ_r^2 at which modelled spectra fit observations. By fitting a paraboloid to the χ_r^2 surface derived in this process (Donati et al. 2003), we can easily infer the magnetic topology that yields the best fit to the data along with the corresponding differential rotation parameters and error bars. This process has proved fairly reliable to estimate surface differential rotation on magnetic stars (e.g., Donati et al. 2003).

3.2 Results

We applied this model to our complete set of Zeeman signatures of τ Boo. Data obtained on the last night (Jul 05), i.e., in bad weather conditions, were finally excluded from

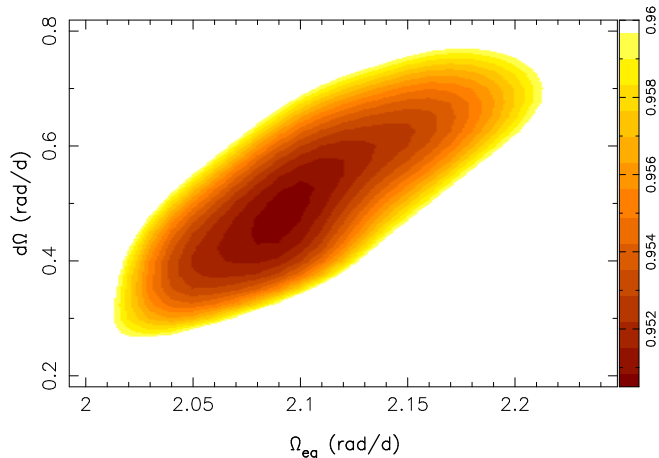


Figure 2. Variation of χ_r^2 as a function of Ω_{eq} and $d\Omega$, derived from the modelling of our Stokes V data set on τ Boo. The outer colour contour corresponds to a 1% increase in χ_r^2 , and trace a 2.7σ interval for each parameter taken separately, or a 1.7σ interval for both parameters as a pair.

the fit as they provide very little information (given their low quality with respect to the bulk of the data set, see Table 1). The rotational broadening of spectral lines provides significant spatial resolution at the surface of the star, i.e., from 9 to 22 resolution elements around the equator depending on whether we use the intrinsic line profile (11 km s^{-1}) or the instrumental profile (4.5 km s^{-1}) to define the resolution element. The spherical harmonics expansions used to describe the magnetic field were first computed up to orders $\ell = 15$; in practice, little improvement is obtained when adding terms with orders higher than 8 in the expansion. All results presented below were thus derived with expansions limited to $\ell = 8$.

The first result from this modelling is that the Stokes V data provide a completely independent confirmation of both the existence and magnitude of differential rotation at the surface of the star, as demonstrated by the well defined χ_r^2 paraboloid we obtain (see Fig. 2). The differential rotation parameters producing an optimal fit to the data (at a given information content in the magnetic map) are respectively equal to $\Omega_{\text{eq}} = 2.10 \pm 0.04 \text{ rad d}^{-1}$ and $d\Omega = 0.50 \pm 0.12 \text{ rad d}^{-1}$ and imply a relative differential rotation of 24%. The corresponding rotation periods at the equator and pole are equal to about 3 d and 3.9 d respectively; the optimal period assuming solid body rotation is 3.23 d and corresponds to the average recurrence time of the detected Zeeman signatures, i.e. to the rotation period at the average latitude (about 35°) of the reconstructed magnetic structures (Donati et al. 2003). The latitudinal surface shear we derive is about 8 to 10 times stronger than that of the Sun; the corresponding timescale for the equator to lap the pole by one complete rotation cycle is only about 12 d.

The large-scale magnetic map we derive (see Fig. 3) corresponds to a unit χ_r^2 fit to the data (see Fig. 4), the initial χ_r^2 being about 1.9 for 750 data points. Note that the evolution of the magnetic field under the shearing effect of differential rotation throughout the period of our observations can be traced directly to the data themselves; for

instance, the Zeeman signature collected at cycle 2.68+245 is significantly smaller in amplitude than those collected 4 rotation cycles later (around cycles 6.70+245).

We find that the field topology includes a small toroidal component enclosing 17% of the overall reconstructed magnetic energy; while the Stokes V data can be fitted without the toroidal component, the corresponding reconstructed map contains significantly more (i.e., +50%) information than that of Fig. 3, suggesting that a purely poloidal field is less probable and that the reconstructed toroidal component is likely real. The toroidal component is clearly visible in Fig. 3 and shows up as ring of positive (i.e., counterclockwise) azimuthal field encircling the star at mid latitude.

The magnetic field is obviously more complex than a dipole, $\ell = 1$ modes enclosing only about 30% of the poloidal field energy. The quadrupolar and octupolar terms (i.e. $\ell = 2$ and $\ell = 3$ modes) dominate the field distribution in the visible hemisphere and contain 40% of the reconstructed poloidal field energy, while the remaining 30% spreads into higher order terms. This is directly visible from Fig. 3; the radial field map features a main positive pole at high latitudes surrounded by an incomplete ring of negative field at low latitudes, reminiscent of a slightly tilted quadrupole or octupole. We also find that the reconstructed poloidal field is mostly axisymmetric with respect to the rotation axis; modes verifying $m < \ell/2$ are enclosing a dominant fraction (i.e. 60%) of the poloidal field energy, while the non axisymmetric modes (with $m > \ell/2$) contain no more than 30% of the poloidal field energy. This is again fairly obvious from the reconstructed map of Fig. 3.

4 DISCUSSION AND CONCLUSION

Thanks to this new data set, we achieved a number of significant results relevant to dynamo processes and magnetic field generation in cool stars with shallow convective zones; We summarise them below and discuss their implications for the study of star/planet magnetic interactions in systems hosting close-in giant planets.

First, we obtained 2 completely independent estimates of the differential rotation at the surface of τ Boo. From the temporal distortion of the large-scale magnetic topology, we find that the latitudinal angular rotation shear is equal to $d\Omega = 0.50 \pm 0.12 \text{ rad d}^{-1}$, i.e., about 8 to 10 times that of the Sun. This is in reasonable agreement with the estimate derived from the detailed shape of spectral lines and of their Fourier transform, yielding $d\Omega = 0.35 \pm 0.10 \text{ rad d}^{-1}$. It unambiguously demonstrates that τ Boo is experiencing strong differential rotation at photospheric level; this is apparently a general trend of early G and F stars (e.g., Marsden et al. 2006; Reiners 2006). Our measurement is also the first direct and simultaneous confirmation that both methods employed up to now to investigate latitudinal shears on stellar surfaces are actually yielding consistent results. The rotation period at the equator of τ Boo is 3 d, i.e., about 10% shorter than the orbital period of the giant planet. It confirms in particular the estimate first obtained by Catala et al. (2007); it also implies that the giant planet is synchronised with the surface of the star at a latitude of about 40° .

We also derived how the magnetic field is distributed at the surface of τ Boo. In particular, we find that the mag-

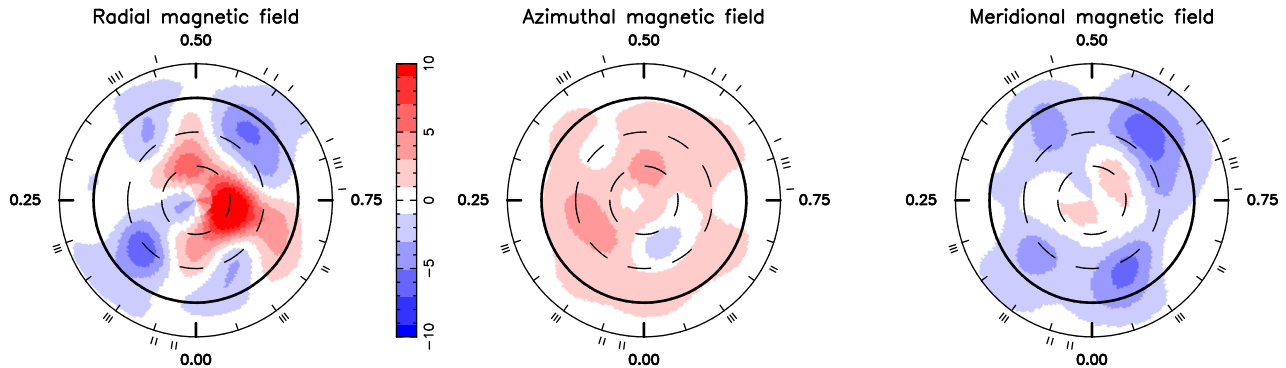


Figure 3. Maximum-entropy reconstructions of the large-scale magnetic topology of τ Boo as derived from our 2007 data set (at orbital cycle 6+245 or HJD 2,454,282.41). The radial, azimuthal and meridional components of the field are displayed from left to right (with magnetic flux values labelled in G). The star is shown in flattened polar projection down to latitudes of -30° , with the equator depicted as a bold circle and parallels as dashed circles. Radial ticks around each plot indicate orbital phases of observations.

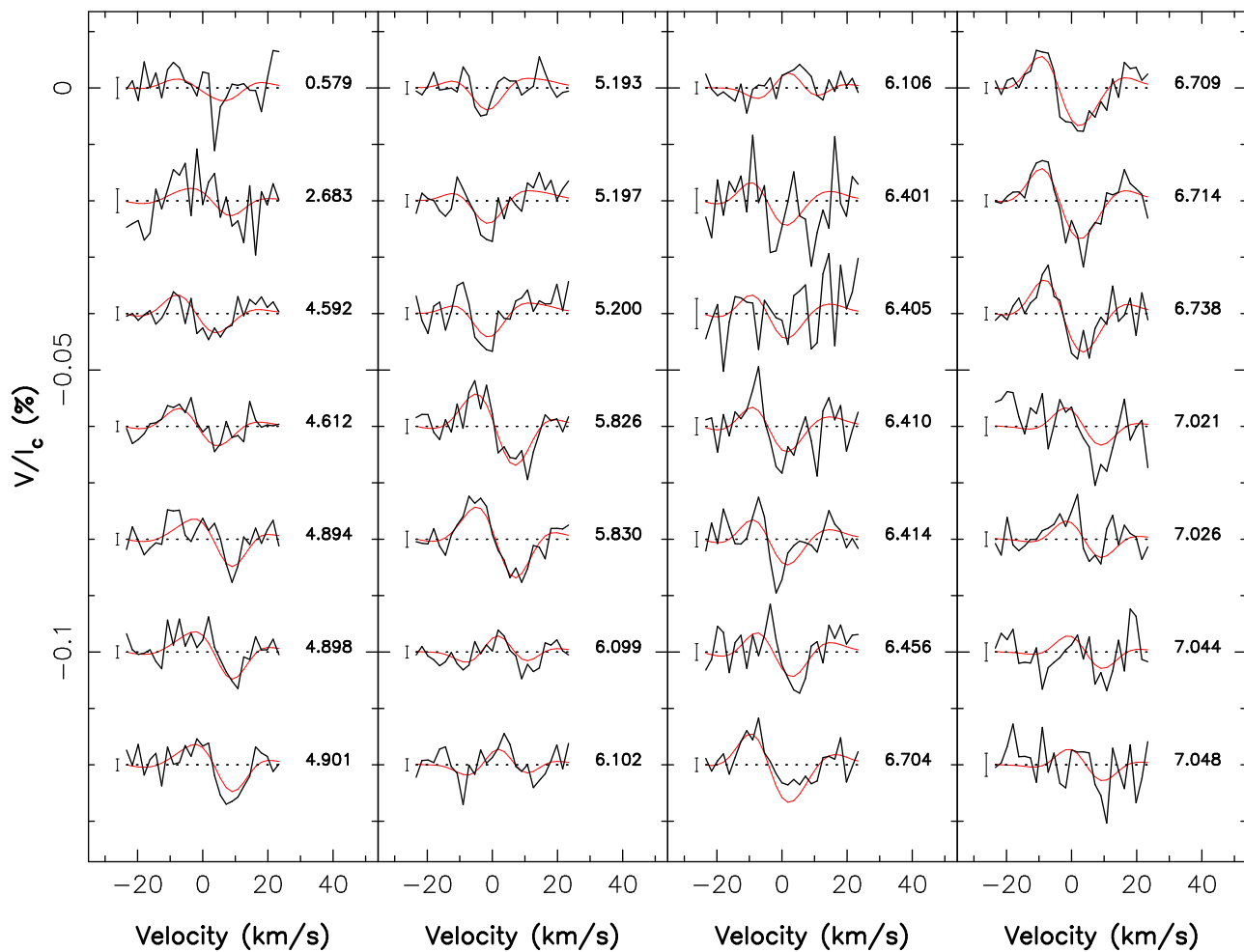


Figure 4. Maximum-entropy fit (thin red line) to the observed Stokes V LSD profiles (thick black line) of τ Boo. The orbital cycle of each observation (as listed in Table 1) and 1σ error bars are also shown next to each profile.

netic field is mostly poloidal despite the vigorous differential rotation. This is different than what Marsden et al. (2006) report for another cool star with a shallow convective zone (HD 171488), in which the magnetic field is apparently distributed roughly evenly between poloidal and toroidal field components; the main difference between both stars is the

rotation rate, less than half as large for τ Boo than for HD 171488. The magnetic topology we reconstruct is grossly similar to (though much more accurate than) that derived by Catala et al. (2007) from a much sparser data set. There is however one major difference between both maps; while the radial field is predominantly positive and negative at

high and low latitudes respectively in our image, the opposite holds in the 2006 image reconstructed by Catala et al. (2007). A similar polarity inversion is observed for the two other field components between the 2006 and 2007 images. Check stars with known magnetic polarities observed during both runs demonstrate that this global polarity switch is not due to instrumental or data reduction problems and can only be attributed to τ Boo itself.

This is the first time that a global magnetic polarity switch is observed in a star other than the Sun. Given that such events are rather unfrequent in the Sun (only once every 11 yr) and have never been detected yet in the 20 or so stars (of various spectral types) that have been observed more than once up to now (e.g., Donati et al. 2003), we speculate that the magnetic cycle of τ Boo is likely shorter than that of the Sun. If the cycle period varies more or less linearly with the strength of differential rotation, we expect the period of the full magnetic cycle (22 yr in the case of the Sun) to be of order 2–3 yr in τ Boo; this argues for renewed and regular spectropolarimetric observations of τ Boo to monitor the evolution of the magnetic field throughout a complete magnetic cycle. Given that the convective zone of τ Boo is very shallow and essentially reduces to a thin layer similar in nature to the solar tachocline (where the magnetic dynamo is expected to operate mostly), our result directly demonstrates that interface dynamos are indeed capable of producing oscillating magnetic topologies.

At this stage, there is not much we can say about activity putatively induced by the presence of the giant planet. There is actually no low-latitude magnetic features either facing the planet (at phase 0.5) or on the other side of the star (phase 0.0), i.e., in regions at which tidal effects are maximum. The main low-latitude magnetic features we detect are the negative radial and meridional field features at phases 0.13, 0.40, 0.60 and 0.93 (see Fig. 3); however, these features are apparently rotating faster than the planet orbital motion (being those from which differential rotation at low latitudes is estimated) and can therefore not be interpreted as due to a putative tidal bulge (rotating in phase with the orbital motion).

We find that activity signatures in usual spectral indexes ($H\alpha$, Ca II H & K, and infrared triplet lines) are very weak, smaller than 0.5% of the unpolarised continuum; they are best visible in $H\alpha$ thanks to the higher spectrum quality around 700 nm (see Fig. 5) and reach a peak to peak amplitude of about 0.2 km s^{-1} (0.44 pm) only. Maximum $H\alpha$ emission (i.e. positive integrals over the residual spectra of Fig. 5) occurs roughly twice per rotation (at phases 0.1 and 0.7) and roughly coincide with the main low-latitude radial field features seen in the magnetic map; we therefore suspect that the two small activity enhancements we detect trace intrinsic activity from the star itself. It is unlikely that this activity is induced by the planet itself through tidal friction (also expected to produce two activity enhancements around phase 0.0 and 0.5); given that the stellar equator is rotating faster than the orbital motion, the tidal bulge is expected to be slightly ahead of the planet (shifted to negative orbital phases), i.e., the opposite of what we actually see. The near synchronisation between the planet orbital motion and the star equatorial rotation (beat period of about 32 d) likely implies that the tidal bulge generates very little friction and features only a marginal misalignment with

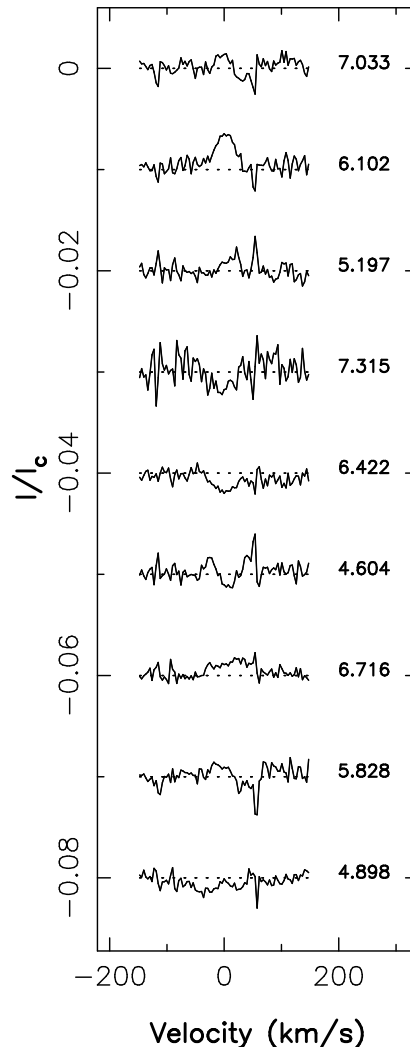


Figure 5. Residual $H\alpha$ signature as a function of orbital cycle. Profiles recorded on the same night were averaged together to reduce noise, and a mean $H\alpha$ profile was subtracted from each nightly average. This operation was performed on ESPaDOnS spectra only. The stray pixels at $+50 \text{ km s}^{-1}$ are due to a weak (and variable) telluric line.

the star-planet direction. Magnetic reconnection triggered by the planet nevertheless remains a potential option for explaining the observed activity variations.

We note that τ Boo is apparently the first convincing case of a star whose rotation is synchronised with the orbital motion of its close-in giant planet. Following Zahn (1994) and Marcy et al. (1997), the synchronisation timescales t_s (in yr) it takes for the planet to enforce corotation of the whole star can be approximated by:

$$t_s = 4.5 \left(\frac{M}{m} \right)^2 \left(\frac{a}{R} \right)^6 \quad (2)$$

where M/m is the star to planet mass ratio (equal to about $350 \sin i$ for τ Boo) and a/R the planet orbit semi-major axis relative to the radius of the star (equal to about 7.2 for τ Boo). Using $i = 40^\circ$, we obtain that $t_s \simeq 30 \text{ Gyr}$, i.e., much larger than the estimated lifetime of τ Boo (about 1 Gyr). Since we consider that the apparent spin-orbit synchronisation between τ Boo and its close-in giant planet is unlikely

to be coincidental, we suspect the synchronisation timescale to be likely overestimated; one possible reason is that synchronisation is not achieved on the whole star (as assumed by Zahn 1994) but only on a restricted volume close to the surface of the star, e.g., the convective zone proper whose mass is estimated to less than 0.1% that of the star. If the tidal effects induced by the close-in giant planet on its host star are strong enough to trigger synchronisation of at least the shallow convective zone, they may also play a significant role in the dynamo processes operating in this thin layer.

More high-quality observations densely sampling the orbital and rotation cycles, carried out over a timescale of typically a month, and repeated at least once a year, are required to go further along these tracks. Such data sets will first allow us to obtain a complete magnetic monitoring of the activity cycle of τ Boo and give us the opportunity to achieve the first such study on a star other than the Sun. These data should also enable us to estimate the lifetime and recurrence rate of the activity enhancements that we detected on τ Boo; if these episodes turn out to be long-lived and synchronised with the orbital motion (rather than with the rotation rate at the stellar equator), they could be unambiguously attributed to the giant planet. Finally, carrying out similar observations on a sample of stars with and without planets to look for statistical differences between both subsamples will also be necessary to investigate in more details the impact of close-in giant planets on the dynamo processes of stars with shallow convective zones.

ACKNOWLEDGMENTS

We thank N. Letourneur and J.-P. Michel for collecting the NARVAL data for us, and the CFHT and TBL staff for their help during the observations. We are grateful to the referee, A. Lanza, for providing comments that improved the manuscript.

REFERENCES

- Butler R. P., Marcy G. W., Williams E., Hauser H., Shirts P., 1997, *ApJ*, 474, L115
- Catala C., Donati J.-F., Shkolnik E., Bohlender D., Alecian E., 2007, *MNRAS*, 374, L42
- Cuntz M., Saar S. H., Musielak Z. E., 2000, *ApJ*, 533, L151
- Donati J.-F., Cameron A., Petit P., 2003, *MNRAS*, 345, 1187
- Donati J.-F., Cameron A., Semel M., Hussain G., Petit P., Carter B., Marsden S., Mengel M., Lopez Ariste A., Jeffers S., Rees D., 2003, *MNRAS*, 345, 1145
- Donati J.-F., Howarth I., Jardine M., Petit P., Catala C., Landstreet J., Bouret J., Alecian E., Barnes J., Forveille T., Paletou F., Manset N., 2006, *MNRAS*, 370, 629
- Donati J.-F., Semel M., Carter B. D., Rees D. E., Collier Cameron A., 1997, *MNRAS*, 291, 658
- Henry G. W., Baliunas S. L., Donahue R. A., Fekel F. C., Soon W., 2000, *ApJ*, 531, 415
- Leigh C., Cameron A., Horne K., Penny A., James D., 2003, *MNRAS*, 344, 1271
- Marcy G., Butler R., Williams E., Bildsten L., Graham J., Ghez A., Jernigan J., 1997, *ApJ*, 481, 926
- Marsden S., Donati J.-F., Semel M., Petit P., Carter B., 2006, *MNRAS*, 370, 468
- McIvor T., Jardine M., Holzwarth V., 2006, *MNRAS*, 367, L1
- Morin J., Donati J.-F., Forveille T., Delfosse X., Dobler W., Petit P., Jardine M. M., Cameron A., Albert L., Manset N., Dintrans B., Chabrier G., Valenti J., 2007, *MNRAS*, in press (astro-ph 0711.1418)
- Moutou C., Donati J.-F., Savalle R., Hussain G., Alecian E., Bouchy F., Catala C., Collier Cameron A., Udry S., Vidal-Madjar A., 2007, *A&A*, 473, 651
- Reiners A., 2006, *A&A*, 446, 267
- Reiners A., Schmitt J., 2002, *A&A*, 384, 155
- Romanova M. M., Lovelace R. V. E., 2006, *ApJ*, 645, L73
- Shkolnik E., Bohlender D., Walker G., Cameron A., 2008, *ApJ*, in press (astro-ph: 0712.0004)
- Shkolnik E., Walker G., Bohlender D., 2003, *ApJ*, 597, 1092
- Shkolnik E., Walker G., Bohlender D., Gu P., Kürster M., 2005, *ApJ*, 622, 1075
- Zahn J.-P., 1994, *A&A*, 288, 829